Physica Scripta. Vol. 58, 481–485, 1998

Dynamics of Ring Dark Solitary Waves in Saturable Self-Defocusing Media

E. D. Eugenieva[1]* and A. A. Dreischuh[2]†

[1] Bulgrian Academy of Sciences, Institute of Electronics, Laboratory on Gas Lasers and Laser Technologies, 72 Tzarigradsko, Chausse Blvd, Sofia 1784, Bulgaria
[2] Max-Plank-Institute for Quantum Optics, Hans-Kopfermann-Str. 1, 85748, Garching, Germany

Received January 16, 1998; revised version received May 2, 1998; accepted June 2, 1998

PACS Ref: 42.65.-k; 42.65.Sf; 42.65.Tg; 42.65.Wi

Abstract

The dynamics of ring dark solitary waves propagating in saturable self-defocusing media is studied numerically. The results show that the saturation leads to a reduction of the ring's transverse velocity when compared to this in Kerr media. At high saturation levels, however, in a formal contradiction but in actual agreement to the one-dimensional case, a strong snake-type instability and creation of optical vortices of alternate topological charges are to be expected.

1. Introduction

Dark spatial solitons (DSSs) propagating in various self-defocusing nonlinear optical materials are subject of intense research in last years [1]. These formations could be characterized as low intensity dips on a uniform background field which do not diffract under propagation and possess a specific phase distribution [2]. The existence of the dark solitons was first predicted by solving the nonlinear Schrödinger equation for a medium of a negative self-defocusing Kerr nonlinearity accounting for the linear effects in one transverse dimension (1D case) [3]. In two transverse dimensions (2D case) such self-supported dark beams were observed experimentally as stripes and grids [4]. The properties of these solitons are similar to the properties of the 1D DSSs. The optical vortex solitons (OVS) are the only "black" spatial solitons of circular symmetry in the 2D space [5, 6]. Characteristic for them is the on-axis screw phase dislocation (helical phase ramp) ensuring zero intensity at the vortex centre. It was shown that the dark soliton stripes are unstable to long-period transverse perturbations [7–10]. When initiated, the instability leads to decay of the dark stripe into multiple pairs of OVSs with alternating topological charges (TCs). This effect is known as snake instability and has been observed in nonlinear media possessing Kerr-type response [10], saturation [11, 12] or photorefractive type of nonlinearity [13, 14].

In bulk nonlinear media another type of solitary waves has also attracted attention – the ring dark solitary waves (RDSWs) [15]. Formally, they can be considered as soliton stripes bent to form a ring. This type of waves has been studied for the case of Kerr-type nonlinear medium. Unfortunately, it was shown that both the ring radius and the soliton contrast vary along the propagation axis [15, 16], thus affecting negatively the guiding properties of these formations.

In view of the potential applications the guiding properties of the DSSs are of significant interest [1]. RDSWs have been proposed for guiding multiple signal beams, thus forming a parallel optical transmission line [17]. Such a device, however, would require stabilization of both the ring radius and the soliton contrast. One possible solution of the problem is to modulate suitably the phase of the background beam bearing the RDSW as suggested in [18]. In this paper we investigate the possibility to suppress the RDSW transverse dynamics by saturating the nonlinearity. The required type of response is observed in alkali metal vapours near a resonance [11] and in photovoltaic and photorefractive crystals [19–21]. For the latter case, however, the model of nonlinearity is more complicated when two transverse dimensions are accounted for [21] and requires a separate consideration lying beyond the scope of the present analysis.

2. Theoretical model

The optical field E was assumed to be slowly-varying and linearly polarized. In a scalar-field paraxial approximation the propagation of a RDSW in a non-linear saturable medium is described by the generalized nonlinear Schrödinger equation (GNSE) [22]:

$$i\frac{\partial u}{\partial z} + \tfrac{1}{2}\Delta_\perp u - \frac{(1+a)|u|^2}{1+a|u|^2}u = 0, \tag{1}$$

where $u = E/\sqrt{I_m}$ is the dimensionless envelope of the electric field, I_m – the maximum background intensity, $a = I_m/I_{sat}$ – the saturation parameter, and I_{sat} stands for the saturation intensity. The maximal nonlinear contribution to the refractive index has the form $\Delta n = n_\infty a/(1+a)$ with $n_\infty = \Delta n(I_m \to \infty)$. In the case of defocusing nonlinearity $n_\infty < 0$. This form of the nonlinear refractive index change corresponds (at $p = 1$) to the more general expression $\Delta n = n_\infty[1 - 1/(1+a)^p]$ used by Kivshar and Afanasjev [23]. The longitudinal scale is introduced by the characteristic nonlinear propagation distance

$$L_{sc} = n_0(1+a)/(-kn_\infty a) = -n_0/(k\,\Delta n), \tag{2}$$

where k is the wave-number inside the medium and n_0 is the linear refractive index. L_{sc} is analogous to the nonlinear

* E-mail: eugenia@phys.uni-sofia.bg
† Permanent address: Sofia University, Department of Physics, 5 J. Bourchier Blvd., Sofia 1164, Bulgaria.

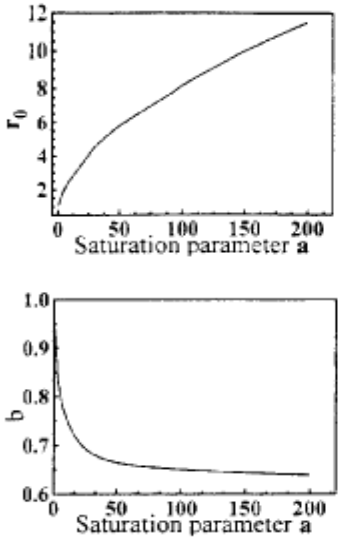

Fig. 1. Plots of the half width r_0 of the dark ring-shaped wave (a) and of the power b of the model tanh function (b) *vs.* saturation parameter (quasi-stationary solution).

length appearing when normalizing the NSE at Kerr nonlinearity. We scaled the transverse coordinates to

$$x_0 = [n_0(1 + a)/(-k^2 n_\infty a)]^{1/2}. \tag{3}$$

In the above notations eq. (1) describes nonlinear beam evolution along a "pure" Kerr-type nonlinear medium (NLM) as $a \to 0$. At high saturation levels ($a \gg 1$) $L_{sc} \to n_0/(kn_\infty)$. The normalization introduced by eq. (2) provides a natural way to compare the propagation distances in these two physically different nonlinear regimes. At all values of the saturation parameter at $z = L_{sc}$ the maximum nonlinear phase shift at the dark beam wings is -1. The transverse scale introduced is similar to the scale used by Valley *et al.* in [19]. We solved eq. (1) numerically by the split-step Fourier method [24] using a mesh of 512 × 512 grid points. The evolution of the RDSWs was studied up to $100L_{sc}$. At the entrance of the NLM ($z = 0$) the field distribution was described by:

$$u = B(r)V(r - R_0) \exp(i\Phi), \tag{4}$$

where

$$B(r) = \exp\{-(r/40)^{10}\}, \tag{5}$$

$$r = (x^2 + y^2)^{1/2}/r_0, \tag{6}$$

$$V(r - R_0) = |\tanh(r - R_0)|^b, \tag{7}$$

x and y being the Cartesian coordinates, and R_0 – the ring radius. The initial phase distribution Φ contains a pair of phase jumps of π in each diametrical cross-section, thus ensuring odd initial conditions for generation of an initially "black" ring-shaped dark beam. The values of r_0 (the ring width) and b were determined by analysing the quasi-stationary solution ($\partial u/\partial z = 0$) of the GNSE for the 1D case at each particular value of the saturation parameter. These solutions were found numerically by using the Runge–Kutta method and were further aproximated with a function of the form

$$|\tanh(x/r_0)|^b. \tag{8}$$

The dependencies of r_0 and b on the saturation parameter a are shown in Fig. 1. We found that values of b other than 1 give a good approximation of the amplitude profile found numerically. Physically this means that at higher saturation levels the wings of the quasi-stationary 1D solution become flatter. In the limiting case $a \to \infty$ no dark solitary-wave formation could be expected since the transverse variations of the refractive index disappear. Note, that r_0 is expressed in units given by eq. (3), i.e. the transverse scale depends on the saturation parameter. The width of the exact solution increases with increasing the saturation and both r_0 and b tend to unity when $a \to 0$ as expected for Kerr type nonlinearity. When the dependence of the scaling lengths on the saturation parameter is removed and b is set to unity the dependence $r_0(a)$ shows the bistability reported in [20, 25].

3. Evolution of the RDSW parameters at different saturation levels

At low saturation ($a \approx 2$ or less) the dark ring radius R_0 and width r_0 are always found to increase as the RDSW propagates along the medium. This results in decrease of the contrast. At certain distance ($z = 30L_{sc}$ for $a = 2$) the dark wave disappears. We found that, similar to the Kerr case [15], the higher the initial ring radius R_0 the lower the transverse ring velocity. This tendency is shown in Fig. 2 for $a = 2$ and should be attributed to the drift instability of dark solitons [22, 23, 26] leading to transformation of the perturbed black solitons into grey ones. At the low saturation considered we do not observe a decay of the RDSW into a chain of optical vortices. In our view this behaviour is due to the nonzero and still saturation-unaffected RDSW transverse velocity. The initially "black" dark ring being expanding, gets more "grey" and more stable (see Ch. 7.5 in Ref. [1]). This regime of propagation, however, is not the proper one for guiding of optical signals within the dark ring-shaped beam because of the high transverse velocities of the RDSW.

Higher saturation levels were found to lead to a reduction of the dark ring transverse velocity as shown in Fig. 3. The contrast of the RDSWs remains relatively high and the same holds for their transverse instability sensitivity. The last statement does not contradict to the general tendency that higher saturation does effectively suppress the DSS transverse instability [1, 12]. As shown in [11, 23] in the regime of strong saturation a "black" 1D DSS transforms into a moving "grey" soliton of lower intensity. In this case the drift instability dominates the transverse instability. In contrast, the saturation of the nonlinearity results in a

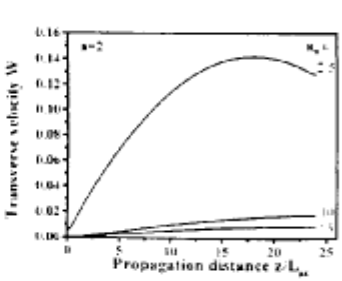

Fig. 2. Normalized transverse velocity $d[R/R_0(z = 0)]/d(z/L_{sc})$ of the RDSW at a low saturation $a = 2$ and different values of the initial ring radius $R_0(z = 0)$.

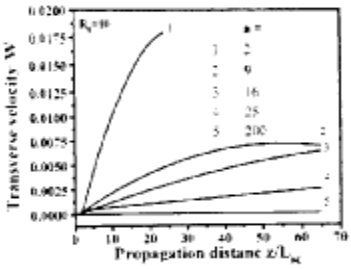

Fig. 3. Normalized transverse velocity $d[R/R_0(z=0)]/d(z/L_{sc})$ of the RDSW at an initial ring radius $R_0(z=0)=10$ for different saturation levels.

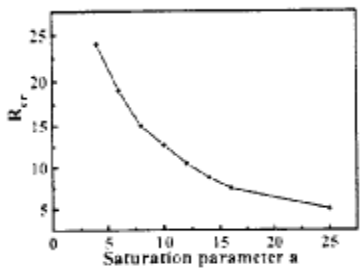

Fig. 5. Dependence of the critical radius R_{cr} for appearance of a snake-type instability vs. saturation parameter.

decrease in the RDSW transverse velocity and it's influence on the RDSW transverse modulational stability reverses. In the following we provide some evidence supporting these conclusions.

In a nonsaturated Kerr medium significant evolution of the ring radius occurs at propagation distances well bellow $10L_{sc}$ [15, 16]. Similar to the previous case, in presence of moderate and high saturation ($a > 4$) the transverse velocity of the RDSW does depend on the initial ring radius $R_0(z = 0)$. This tendency is clearly expressed in Fig. 4, but it becomes significant at higher propagation distances ($z/L_{sc} > 10$). It could be inferred from Fig. 3 and Fig. 4 that higher saturation levels and larger initial ring radii $R_0(z = 0)$ result in a stabilization of the ring radius and contrast and, therefore, the RDSW guiding properties should be better preserved. Our further analysis showed, however, that at saturation levels of $a = 4$ or more the RDSW evolution becomes crucially dependent on the initial ring radius $R_0(z = 0)$. At these levels there exists a critical value R_{cr} of the initial ring radius. At $R_0(z = 0) < R_{cr}$ the ring radius increases along the propagation path in the nonlinear medium and the soliton contrast decreases accordingly (drift instability; [22, 23]). At $R_0 > R_{cr}$ the ring initially expands slightly and the typical snake-type instability develops. At higher initial ring radii the creation of pairs of optical vortex solitons (OVSs) of alternating topological charges was clearly expressed. Such behaviour seems to be analogous to the instability of the dark soliton stripes against long-period transverse perturbations. Qualitatively, the ring symmetry remains always preserved. The dependence of the critical dark ring radius R_{cr} on the saturation parameter a is shown in Fig. 5. Since R_{cr} increases with decreasing saturation a, it should be expected that the critical radius for observation of snake instability in Kerr case is relatively large. This could be the reason for the fact that such kind of instabilities have been observed experimentally in presence of saturation only

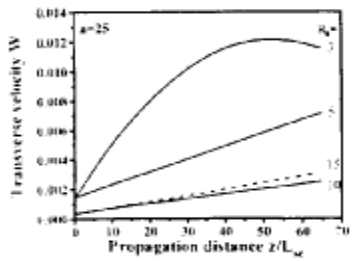

Fig. 4. The same as in Fig. 2 at moderate saturation $a = 25$ and different values of the initial ring radius $R_0(z = 0)$.

[12, 14]. The existence of a critical value of the initial ring radius could be explained in the following way. At $R_0 < R_{cr}$ the drift instability of dark solitons [22, 23] dominates leading to a decrease of the soliton contrast. Since the "gray" solitons exhibit higher stability to transverse perturbations [9], snake-type instability and creation of OVS pairs should not be expected. The ring evolution is a result from the transverse spatial drift mainly.

At $R_0 > R_{cr}$ the contrast of the dark ring remains relatively high and two mechanisms of dark soliton instability should be accounted for – the drift instability and the instability of a (bent) dark stripe against transverse perturbations [9]. For the case of Kerr-type nonlinearity the number of OVS pairs created could be associated with the period T_{cr} of the transverse perturbation which causes instability of a dark soliton stripe [8, 13]. It was shown that the evolution of a dark stripe in the presence of transverse perturbations depends on the perturbation type [8]. Law and Swartzlander reported that filtering of the soliton field through a long-period grating results in subsequent creation OVS pairs at different propagation path lengths. As could be seen in Fig. 6 similar subsequent creation of OVS pairs under RDSW propagation in a saturable medium takes place. We clearly observed also interaction in- and between the OVS-pairs by comparing their spatial positions at different propagation path-lengths. Considering the initial dark ring as a bent stipe, obviously the initial dark formation is a subject of non-negligible perturbations. Figure 6 shows the evolution of a RDSW at $a = 25$ and $R_0 = 15r_0 > R_{cr}$ up to $z = 100L_{sc}$. The phase distribution of the optical field suggests an azimuthal phase change of 2π in the vicinity of the dark spots which is the characteristic of OVSs. Note, that for two adjacent spots the phase change has opposite gradients. Similar behaviour was observed at a moderate saturation of a ($a \approx 10$). Each 90-degree pie-part of the dark ring was found to decay in the same manner under the instability independent on the particular number of the vortices generated. At very high saturation levels ($a \approx 200$) the snake-type instability was always present, but at distances between the adjacent vortices of the order of the vortex radius. This behaviour is demonstrated in Fig. 7. The phase distribution of the optical field, however, is indicative for the creation of such pairs of optical vortices. The small distance between the centers of optical vortices could be associated with the increased stability of a DSS against transverse perturbation at strong saturation regime [12].

The waveguiding properties of the DSS are well known [1]. This suggest the idea that the splitting of the initial RDSW during its propagation in saturable self-defocusing

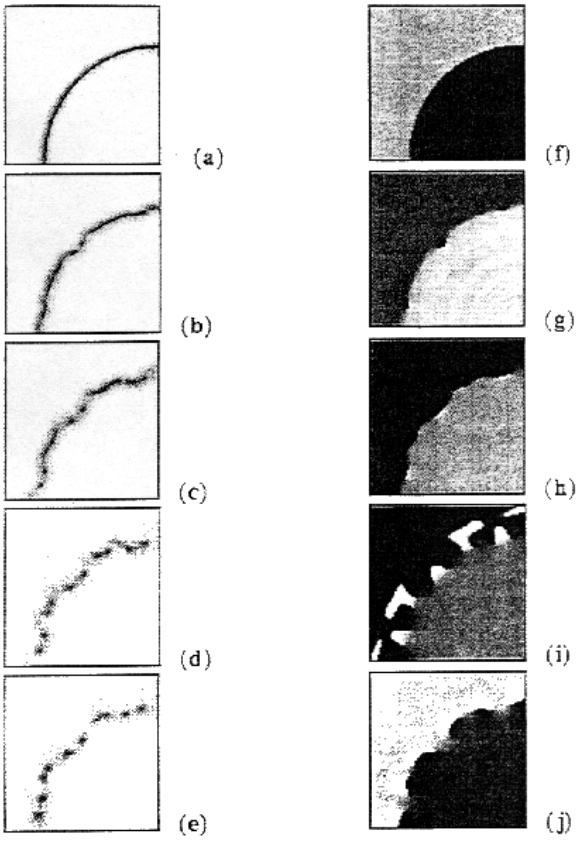

Fig. 6. Gray-scale image of the intensity (a–e) and phase (f–j) distribution of optical field at $a = 25$, $R_0 = 15$ and $z = 0$ (a, f), $z = 40$ (b, g), $z = 60$ (c, h), $z = 80$ (d, i), $z = 100$ (e, j). Black points in the phase portraits correspond to a phase of $-\pi$, white points – to π. Only 2.8% of the total computational window are presented.

media could be used for branching of optical signals guided by the ring dark wave into discrete number of channels formed by the OVSs created. In view of the above results the most proper range of operation for such a brancher are the values of the saturation parameter a between 5 and 25. For lower values of a it would be difficult to force the initial dark wave to split. For higher saturations the width of the initial dark ring would be too large thus suggesting a multimode waveguiding at the initial evolution stage (undesired for photonic applications). Having in mind that only part of the ring is needed to form OVSs it could be suggested that a bent stripe of a proper curvature could be used to form the desired number of optical vortices. Since R_{cr} is relatively large for moderate saturation parameters it could be expected that a stripe of relatively short length and large curvature could be used in order to create OVSs and therefore a photonic splitter. This splitting mechanism could be used for writing a photonic brancher in photovoltaic crystals despite of the anisotopy of optical nonlinearity. The behaviour of optical vortices in such crystals, however, is rather complicated [27] and the above idea requires further extensive studies.

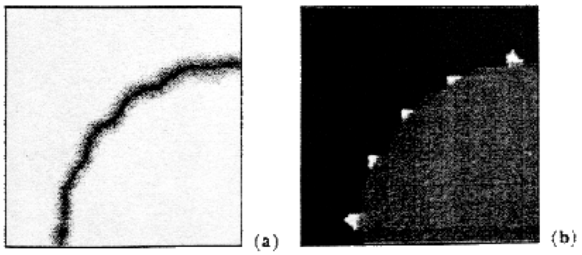

Fig. 7. Pie-parts of the gray-scale encoded images of the intensity (a) and phase (b) distribution of the optical field at $a = 200$, $R_0 = 10$, and $z = 80$.

Our results show that for saturation parameters a ranging from 5 to 25 the propagation distances at which the optical vortices are well separated, are of the order of $z \approx 80L_{sc}$ or less. The required maximal nonlinear contribution to the refractive index could be estimated by using eq. (2) $|\Delta n| = 80n_0/(kz)$. This suggests that for $z = 2$ mm the required nonlinear contribution is $\Delta n = 7 \times 10^{-3}$ at an optical wavelength of $\lambda = 0.5\,\mu$m and $n_0 = 2.2$ ($LiWbO_3$). Such a value of the nonlinear refractive index is accessible experimentally in the presence of the saturation of the nonlinearity.

4. Conclusion

The dynamics of the ring dark solitary waves in saturable nonlinear optical media was studied numerically in order to estimate the possibility to suppress their transverse dynamics by saturating the optical nonlinearity. As a result of the development of a snake-type instability at some saturation levels we observed splitting of the initial dark ring into chains of OVSs with alternating topological charges. A proper range of the saturation parameters is suggested for forming a photonic brancher in this regime.

Acknowledgement

E.E. would like to thank to Mr. D. Neshev for the helpful discussions. A.D. would lke to thank to the Alexander von Humboldt-Stiftung for the awarded fellowship and for the possibility to work in the exiting atmosphere of the Max-Planck-Institut für Quantenoptik (Garching, Germany).

References

1. Kivshar, Yu. S. and Luther-Davies, B., "Dark Solitons in Nonlinear Optics", Phys. Reports **298**, 81 (1998), and references therein.
2. Kivshar, Yu. S., IEEE J. Quant. Electron. **29**, 250 (1993).
3. Zakharov, V. and Shabat, A., Sov. Phys. JETP **37**, 823 (1973) [in Russian: Zh. Eksp. Teor. Fiz. **64**, 1627 (1973)].
4. Swartzlander, G. A., Andersen, D. R., Regan, J. J., Yin, H. and Kaplan, A. E., Phys. Rev. Lett. **66**, 1583 (1991).
5. Snyder, A. W., Poladian, L. and Mitchel, D., Opt. Lett. **17**, 789 (1992).
6. Swartzlander, G. A. and Law, C. T., Phys. Rev. Lett. **69**, 2503 (1992).
7. Kuznetsov, E. A. and Turitsyn, S. K., Zh. Eksp. Teor. Fiz. **94**, 119 (1988).
8. Law, C. T. and Swartzlander, G. A., Opt. Lett. **18**, 586 (1993).
9. Pelinovski, D. E., Stepanyants, Yu. A. and Kivshar, Yu. S., Phys. Rev. **E51**, 5016 (1995).
10. McDonald, G. S., Syed, K. S. and Firth, E. J., Opt. Commun. **95**, 281 (1993).
11. Tikhonenko, V., Christou, J., Luther-Davies, B. and Kivshar, Yu. S., Opt. Lett. **21**, 1129 (1996).
12. Luther-Davies, B., Christou, J., Tikhonenko, V. and Kivshar, Yu. S., J. Opt. Soc. Am. **B14**, 3045 (1997).
13. Manaev, A. V., Saffman, I. and Zozulya, A. A., Phys. Rev. Lett. **76**, 2262 (1996).
14. Mamaev, A. V., Saffman, I. and Zozulya, A. A., Phys. Rev. **A54**, 870 (1996).
15. Kivshar, Yu. S. and Yang, X., Phys. Rev. **E50**, R40 (1994).
16. Neshev, D. *et al.*, Appl. Phys. **B64**, 429 (1997).
17. Dreishuh, A., Kamenov, V. and Dinev, S., Appl. Phys. **B63**, 145 (1996).

18. Kamenov, V., Dreischuh, A. and Dinev, S., Physica Scripta **55**, 68 (1997).
19. Valley, G. *et al.*, Phys. Rev. **A50**, R4457 (1994).
20. Segev, M., Valley, G., Bashaw, M. C., Taya, M. and Fejer M. M., J. Opt. Soc. Am. **B13**, 1772 (1997).
21. Zozulya, A. A. and Anderson, D. Z., Phys. Rev. **A51**, 1520 (1995).
22. Pelinovski, D. E., Kivshar, Yu. S. and Afanasjev, V. V., Phys. Rev. **E54**, 2015 (1996).
23. Kivshar, Yu. S. and Avanasjev, V. V., Opt. Lett. **21**, 135 (1996).
24. Agrawal, G. P., "Nonlinear Fiber Optics" (Academic: Boston, MA), chap. 2 (1989).
25. Gatz, S. and Hermann, J., J. Opt. Soc. Am. **B8**, 2296 (1991).
26. Kivshar, Yu. S. and Krolikowski, W., Opt. Lett. **20**, 1527 (1995).
27. Mamaev, A. V., Saffnam, I. and Zozulya, A. A., Phys. Rev. **A56**, R1713 (1997).